Pacific Ocean Heat Transport at 24°N in a High-Resolution Global Model

JOHN L. WILKIN, JAMES V. MANSBRIDGE, AND J. STUART GODFREY

CSIRO Division of Oceanography, Hobart, Tasmania, Australia

(Manuscript received 11 July 1994, in final form 9 November 1994)

ABSTRACT

Meridional heat transport in the North Pacific Ocean in a seasonally forced high-resolution global ocean general circulation model is compared to observations. At 24°N, annual mean heat transport in the model of 0.37×10^{15} W is half the most recent direct estimate of $0.76 \pm 0.3 \times 10^{15}$ W from hydrographic data. The model value is low because the model ocean loses too little heat in the region of the Kuroshio Current Extension. The water ventilated in this region returns southward across 24°N at depth between 200 m and 500 m approximately 2°–4°C too warm. If the model surface temperature were relaxed to a temperature adjusted for the influence of persistent atmospheric cooling in this region, rather than relaxed to climatological sea surface temperature, the model heat transport would improve.

Assumptions inherent in estimating meridional heat transport from hydrographic sections are tested by examining the model. Rather than the abyssal circulation being steady, the model's deep western boundary currents vary seasonally to balance the seasonal cycle of Ekman transport, producing a larger seasonal variation in heat transport than is generally supposed for direct heat flux calculations. But the variability is such that there is no net contribution to the mean heat transport through a seasonal correlation between winds and surface temperature. The use of surface temperature observed during a single hydrographic section can seasonally bias an estimate of the wind-driven component of the heat transport, so a modification is proposed to the procedure by which compensation is made for seasonal variability in direct heat transport calculations. The most recent direct estimate was based on a springtime section, for which the model heat transport would be underestimated by about 0.05×10^{15} W.

Interannual timescale correlations in the transport and temperature of the Kuroshio Current contribute a net southward transport of some 0.07×10^{15} W. The role of simulated mesoscale eddies is minor.

Given the comparable order of the southward interannual heat transport and the northward seasonal bias, this present study does not suggest any significant revision to the latest direct heat transport estimate for 24°N in the Pacific.

Other features of the model general circulation are noted, including a Kuroshio Current transport that is stronger than observed and the persistence of a branch of the Kuroshio that does not separate at 35°N but continues close to the coast forming unrealistically deep mixed layers through intense surface cooling.

1. Introduction

A major component of present climate research, especially within the World Ocean Circulation Experiment (WOCE) community, concerns the development of ocean circulation models for climate simulation and prediction and the comparison of these models with observations. The purpose of model–data comparisons is not solely to determine whether a model has performed well or poorly or to identify which features of a particular model need most urgent improvement. They also provide a test of the validity of the assumptions that underlie the calculation of, for example, oceanic meridional heat transport from hydrographic and other observable ocean properties, and can therefore assist in improving the interpretation of observations. Furthermore, models readily provide information on the seasonal cycle of the oceanic heat budget, which is often difficult to obtain directly because of limitations on observational resources.

The comparison presented here focuses on meridional heat transport at latitude 24°N in the Pacific Ocean. The heat and mass transport simulated by a high-resolution global ocean model (Semtner and Chervin 1992) are compared to a high-resolution trans-pacific hydrographic survey (Bryden et al. 1991) of the type being conducted globally as part of WOCE.

The Pacific 24°N section was chosen for particular attention for the following reasons. The oceanic contribution to global meridional heat transport is large at this latitude, and it is therefore critical that models perform well here in order to achieve realistic simulations of the global climate. Compared to the North Atlantic Ocean, Pacific heat transport is relatively poorly known. This is due to the vast size of the ocean and the consequent low density of ship observations from which estimates of the heat budget might be

Corresponding author address: Dr. John L. Wilkin, Division of Oceanography, CSIRO, GPO Box 1538, Hobart, Tasmania 7001, Australia.
E-mail: wilkin@flood.ml.csiro.av

computed from air–sea fluxes. The expanse of the Pacific has also conspired against the commitment of resources to more than a handful of zonal hydrographic sections.

The North Pacific also differs fundamentally from the Atlantic in its principal mode of heat transport. Atlantic heat transport is dominated by the exchange of northward flowing surface and thermocline waters and the southward export of cold North Atlantic Deep Water. No deep water is formed in the North Pacific, so the abyssal circulation does not contribute significantly to the mean heat transport (Bryden 1993). Because of this feature, it was anticipated that an ocean model driven with mean seasonal winds and surface fluxes, and having good resolution of the upper thermocline and surface waters, should provide a reasonable simulation suitable for examining the North Pacific heat budget. A model with resolution sufficient to allow the formation of mesoscale eddies would enable the examination of their role in the heat budget. For these reasons, the model of Semtner and Chervin (1992) was chosen for the present study.

2. Pacific Ocean heat transport observations

Observations of the annual mean meridional heat transport in the North Pacific were summarized by Talley (1984). Indirect estimates, obtained by integrating from north to south the air–sea heat flux given by meteorological bulk formulae applied to surface observations, showed widely varying results. Talley (1984) concluded that systematic errors in the bulk parameterizations were too large to give a confident estimate of the total heat transport at any latitude in the Pacific. Even the sign of this transport was in doubt when systematic errors of order ± 10 W m^{-2} in each component of the air–sea flux (which would integrate to $\pm 0.5 \times 10^{15}$ W over the North Pacific) were acknowledged. At 24°N, Talley's (1984) analysis of ship observations gave a northward transport of just 0.002 petawatts (1 PW = 10^{15} W). This is considerably lower than another indirect estimate of 0.74 PW by Esbensen and Kushnir (1981). Talley also reviewed estimates of oceanic transport based on the residual difference between net radiation at the top of the atmosphere and atmospheric heat transport (Hastenrath 1980), and a direct estimate using hydrographic data at 35°N by Bryan (1962). In Fig. 1 we show the data reviewed by Talley and add the results from studies conducted since her review was published. These include an indirect estimate computed from Oberhuber's (1988) analysis of the COADS (Comprehensive Ocean–Atmosphere Data Set) data, the residual oceanic transport inferred by Trenberth and Solomon (1994) from the earth's radiation budget and atmospheric transport in a forecast model, and a direct estimate from hydrographic data at 24°N by Bryden et al. (1991), hereafter referred to as BRC. These recent studies give meridional heat transport estimates at 24°N of, respectively, 0.79 ± 0.3 PW, 0.96 ± 0.18 PW, and 0.76 ± 0.3 PW. (Oberhuber did not give error estimates, so the value quoted here is based on Talley's estimate of typical errors in indirect methods.) Also shown is a direct estimate by McBean (1991) of 1.0 ± 0.5 PW at 35°N.

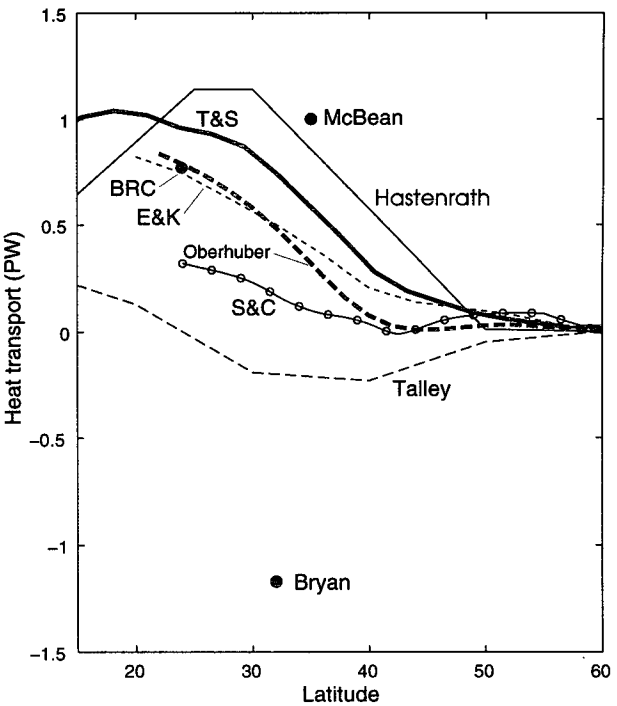

FIG. 1. Annual mean meridional heat transport in the North Pacific Ocean. Talley (1984) (light dashed line), Esbensen and Kushnir (1981) (light dotted line), and Oberhuber (1988) (heavy dashed line) indirect estimates from air–sea flux data. Hastenrath (1980) (light solid line) and Trenberth and Solomon (1994) (heavy solid line) residual of radiation budget and atmospheric transport. Bryan (1962), Bryden et al. (1991) (BRC), and McBean (1991) direct hydrographic estimates. Meridional integral of Semtner and Chervin (1992) model surface heat flux (solid line with circles).

a. *Direct estimation of heat transport*

The great advantage of direct estimates when examining results from an ocean model is that they provide not only an estimate of the total meridional heat transport, but how this transport is distributed as a function of temperature, and the relative contributions of different dynamic processes.

Direct estimates of ocean heat transport are made by integrating across a vertical section the product of mass transport and heat content. This may be written

$$F = \int\int \rho c_p v \theta \, dx dz, \qquad (1)$$

where v is the velocity normal to the section, θ the potential temperature, and ρ and c_p are the density and specific heat of seawater. To make their calculation,

BRC used geostrophic velocities computed from the 24°N section hydrography plus an Ekman component calculated using annual mean winds from the climatology of Hellerman and Rosenstein (1983). Mass must be conserved across the section for the estimate to be independent of the temperature scale, so BRC assumed there was no transport through the Bering Strait. The effect on the heat transport calculation of assumptions made in referencing the geostrophic velocities and incorporating the annual mean wind-driven component are examined later.

In their analysis, BRC follow the approach of Hall and Bryden (1982) and split the heat transport into three components: the western boundary current (Kuroshio Current), the Ekman transport, and a midocean geostrophic flow:

$$F = \rho c_p \left(\int\int_K v_K \theta_K dx dz + \int\int_E v_E \theta_E dx dz + \int\int_G v_G \theta_G dx dz \right). \quad (2)$$

(The product $\rho c_p = 4.06 \times 10^6$ J m^{-3} °C^{-1} may be taken outside the integration because it is constant within the order of accuracy of the calculations.) Dividing each term above by the respective volume flux, $V = \int\int v dx dz$, gives a transport-weighted mean temperature Θ for that component of the circulation, so that the total heat flux may be written

$$F = \rho c_p (V_K \Theta_K + V_E \Theta_E + V_G \Theta_G). \quad (3)$$

Noting that the net volume transport is zero, (3) may be written

$$F = \rho c_p [V_K (\Theta_K - \Theta_G) + V_E (\Theta_E - \Theta_G)]. \quad (4)$$

This emphasizes that the heat transport occurs due to northward transport of water at one temperature being returned southward at another. By this procedure, BRC calculate a total heat transport of 0.76 PW distributed almost equally between the Kuroshio (0.39 PW) and Ekman (0.37 PW) components. This decomposition into components, and the distribution of heat transport with temperature class and depth are compared to the model heat transport in the next section.

Further information on how mass and heat transports are distributed in the midocean geostrophic component are available from the study of Roemmich and McCallister (1989). Using four meridional and three zonal hydrographic sections (including 24°N) and other data, they computed an inversion of the North Pacific mean circulation by applying conservation constraints to the mass budget in several density layers. In the next section we also examine the distribution with longitude of the model mass transport across 24°N, and the North Pacific abyssal circulation, in light of Roemmich and McCallister's (1989) results.

3. Model heat transport

a. Model description

The global ocean general circulation model results examined here are from the study of Semtner and Chervin (1992). The model has a horizontal resolution of 0.5° lat × 0.5° long and 20 vertical levels. It was driven with monthly winds from the climatology of Hellerman and Rosenstein (1983) and surface fluxes parameterized by relaxing model surface salinity (S) and temperature to observed seasonal surface values (Levitus 1982) with a 30-day timescale relaxation coefficient (equivalent to 40 W m^{-2} °C^{-1} for the model's 25-m thick surface layer). Deep S and θ (below 710-m depth) were relaxed weakly (3-year timescale) to annual mean observed values, as were S and θ at all depths within 10° of latitude of the northern and southern boundaries.

The results we analyze here are monthly ensemble means for the last 5 years of 10-year integration with seasonally varying forcing; that is, monthly means for 5 years were computed and the five realizations of each month averaged to form each ensemble. The initial condition for the seasonal run was the model state after 22.5 years of integration with climatological annual mean forcing. The history of the model run is described in detail by Semtner and Chervin (1992).

In formulating the model geometry, the bathymetry was smoothed and some coastline details altered. In the North Pacific, the model western boundary follows the continental shelf break from Taiwan to Japan, and the Kuril Islands to Kamchatka, thereby removing the East China, Japan, and Okhotsk Seas. Some effects of these simplifications are discussed later. The Bering Strait is closed so that the net meridional mass transport in the North Pacific is zero.

The model's global heat budget was examined by McCann et al. (1994) who tested that the model had achieved thermodynamic equilibrium by comparing two 3-year periods of the seasonal forcing run. For the Pacific at 15°N they found temperature transports in the layers above 710-m depth differed by less than 1% between years 5–7 and years 8–10 (see McCann's et al. Figs. 6 and 7). On the basis of these results, we conclude that the North Pacific heat budget may be considered stationary over the 5-year averaging period considered here.

b. Net heat transport: Annual mean results

The annual mean heat transport across 24°N in the model is 0.37 PW. This is half the BRC estimate of 0.76 ± 0.3 PW. We will show that this discrepancy results primarily from insufficient air–sea heat loss from the model ocean in the Kuroshio Current Extension. However, the model estimate includes time variability, and this accounts for part of the difference.

TABLE 1. Contributions to model annual mean heat transport (10^{15} W) on different timescales.

Total $\overline{\langle v\theta \rangle}$	Steady circulation $\langle \overline{v} \rangle \langle \overline{\theta} \rangle$	Interannual variation $\overline{\langle v \rangle'' \langle \theta \rangle''}$	Monthly variation $\overline{\langle v \rangle^* \langle \theta \rangle^*}$	Eddy variation $\overline{\langle v'\theta' \rangle}$
0.371	0.459	−0.0707	−0.0028	−0.0147

Denoting the monthly ensemble model statistics by angle brackets, and the annual mean of these by an overbar, the annual mean model temperature flux is $\overline{\langle v\theta \rangle}$. This is made up of contributions on several timescales. The temperature flux due to the 5-year mean velocity advecting the 5-year mean temperature is $\langle \overline{v} \rangle \langle \overline{\theta} \rangle$. Denoting the departure of the instantaneous solution from each monthly mean by a prime, the term $\overline{\langle v'\theta' \rangle}$ represents the temperature flux due to mesoscale eddy fluctuations occurring on a timescale of less than 30 days. Similarly, denoting the departure of the monthly ensembles from the 5-year mean by an asterisk, the correlation between monthly variation in v and θ contributes $\overline{\langle v \rangle^* \langle \theta \rangle^*}$ to the net temperature flux, and a further term $\overline{\langle v \rangle'' \langle \theta \rangle''}$ represents interannual correlations. This decomposition of the heat transport is shown in Table 1.

The assumption in the Hall and Bryden (1982) method that velocity and temperature estimated from the hydrographic section are representative of the annual mean suggests that BRC's estimate is most appropriately compared to $\langle \overline{v} \rangle \langle \overline{\theta} \rangle$, which for the model is 0.46 PW, just within the error bounds of BRC's value. Mesoscale eddy variability contributes less than 3% to the total heat transport. Though monthly variations in v and θ are large, they are not correlated in such a way as to produce a significant contribution to the mean heat budget. Monthly variation is discussed in more detail in the section on annual variability.

Interannual correlations produce a southward heat transport of 0.0707 PW, which is of order 20% of the total but in the opposite direction. This contribution arises entirely from variations in the core of the Kuroshio Current between 100-m and 500-m depth. Time series and power spectra of transport and temperature in the model (Semtner and Chervin 1992, their Figs. 20 and 22) show the Kuroshio transport is one of the features that exhibits the largest interannual variation. A southward heat transport implies increased Kuroshio transport anomalies are correlated with cool temperature anomalies. However, this term is calculated from a model average taken over only 5 years and therefore may not constitute a robust estimate of model interannual variability.

Notwithstanding the significant underestimation of the net heat transport, there are several useful results to be deduced by examining the model heat transport components in the same manner as BRC.

c. *Components of the heat transport*

The BRC section departs from 24°N latitude at the eastern boundary, the Hawaii Ridge, and the western boundary where it crosses the Kuroshio Current in the Okinawa Trough. In the model analysis we follow 24°N for the entire section, and therefore consider the Kuroshio Current where it is adjacent to the Taiwan coast.

BRC used velocities computed from hydrography assuming geostrophy, plus an ageostrophic wind-driven component. We treat the velocities computed by the model, after subtraction of the Ekman component, as "geostrophic," although they potentially include other ageostrophic processes. The role of reference level assumptions on BRC's results is discussed later.

1) WESTERN BOUNDARY CURRENT

At 24°N the model Kuroshio flows northward between Taiwan and 126°E transporting 51.2 Sv (Sv $\equiv 10^6$ m^3 s^{-1}) in the annual mean at an average temperature of 18.48°C. This temperature is practically identical to BRC's estimate (Table 2). A strong recirculation returns 12 Sv southward between 126° and 132°E for a total northward transport of 40 Sv. This transport is comparable to estimates of 52.4 Sv for the Kuroshio and 18.1 Sv for the recirculation (total 33.0 Sv) from repeated hydrographic sections along 137°E (Qiu and Joyce 1992), and Roemmich and McCallister's (1989) total 43.8 Sv (Table 3) across 24°N west of 137°E. In keeping with BRC's approach, we include the recirculation with the midocean geostrophic component rather than the Kuroshio component and contrast the model 51.2 Sv with BRC's Okinawa Trough transport of 28.3 Sv. Why should these values differ by so much? Since the combined model transport of the Kuroshio and its recirculation are within the range of observations, the model recirculation must be too vigorous. This is possible because smoothing of the model bathymetry set the Tokara Strait sill depth to 710 m, rather than 550 m or shallower, and eliminated

TABLE 2. Net heat transport across 24°N in the Pacific.

	Bryden et al. (1991)		Model	
	Transport (Sv)	Temperature (°C)	Transport (Sv)	Temperature (°C)
Ekman	12.0	22.56	12.7	24.91
Kuroshio	28.3	18.46	51.2	18.48
Midocean	−40.3	15.11	−63.9	18.34
	Temperature difference (°C)	Heat transport (PW)	Temperature difference (°C)	Heat transport (PW)
Ekman	7.45	0.37	6.57	0.34
Kuroshio	3.35	0.39	0.14	0.03
Total		0.76		0.37

TABLE 3. Geostrophic transport across 24°N in selected longitude ranges. Results from Roemmich and McCallister's (1989) inversion of North Pacific circulation are for their "model IA."

Longitude range	Transport (Sv)			
	Model		Roemmich and McCallister	
West boundary–Ryukyu Island	51.2	39.4	30.7	43.8
Ryukyu Island–137°E	−11.8		13.1	
137°E–Izu Ridge	−1.8		12.6	
Izu Ridge–152°E	3.2	−19.6	−49.9	−23.4
152°E–175°W	−18.6		25.4	
175°W–Hawaii	−2.5		−11.5	
Hawaii–152°W	−6.9	−32.5	−16.5	−30.9
152°W–east boundary	−25.7		−14.4	
Total (balanced by Ekman)		12.7		−10.6

the Ryukyu Islands altogether, thereby reducing topographic drag. Bingham and Talley's (1991) analysis of the BRC data shows the Okinawa Trough transport includes southward flow immediately west of Okinawa (their Fig. 1). Had BRC reported the strictly northward transport of the Kuroshio their value would therefore be somewhat greater. Thus, while the comparison of model and observed Kuroshio mass transport is at first disappointing, it does not indicate any major shortcoming of the simulation, and only "colors" somewhat the interpretation of the relative contribution of the western boundary component.

2) EKMAN LAYER

The model mixed layer dynamics are simple: Wind stress is applied as a body force to the surfacemost level of the model (0–25-m depth) producing a slablike Ekman layer. Accordingly, we take the Ekman component temperature to be the model θ at 12.5-m depth. BRC assume the Ekman velocity decreases linearly from the surface to 50 m and weight observed θ differently to compute Θ_E. The two approaches do not differ significantly; if the temperature profile were linear, BRC's average temperature would coincide with the observed at 16.5-m depth.

The model mean Ekman transport across 24°N is 12.7 Sv at an average temperature of 24.91°C, compared to BRC's 12.0 Sv at 22.56°C. The model and BRC use the same winds and similar Ekman dynamics, so agreement in the mass transport is expected with minor differences occurring because we consider a strictly 24°N path, and the monthly wind climatology was spline interpolated to three-daily values to force the model.

The difference in Θ_E occurs because of seasonal variability. The 24°N section was occupied during April and May. BRC make partial allowance for this by using annual mean winds to compute V_E, but make no allowance for variability in Ekman layer temperature. Along 24°N, observed sea surface temperature (SST) in April–May is typically 1°C cooler than in the annual mean (Fig. 2). This difference is reflected in the model April–May transport-weighted temperature (Θ_E) being 1.3°C cooler at 23.6°C. BRC use their observed θ because they require an Ekman layer θ, not just SST. If the observed Θ_E were increased about 1°C to give a value more representative of the annual mean, this would increase BRC's heat flux for this component from 0.37 to 0.42 PW.

We also note that during other months SST is even further removed from the annual mean (Fig. 2). Using θ observed in a single hydrographic section without regard for seasonal variability could lead to substantial errors in the Ekman component of any direct heat transport calculation.

3) MIDOCEAN GEOSTROPHIC FLOW

The combined Ekman and Kuroshio components are balanced in the model by a southward midocean flow of 63.9 Sv at an average temperature of 18.3°C, well above BRC's value of 15.11°C. Of this, 32.5 Sv returns south between North America and the Hawaii Ridge (compared to 21.6 Sv according to BRC); 17.8 Sv returns south between the Hawaii and Izu–Ogasawara Ridges (cf. 27.4 Sv); and 13.6 Sv southward between the Izu–Ogasawara Ridge and the Ryukyu Islands (cf. 8.8 Sv *northward*). The return flow is stronger than observed throughout the section, but particularly so in the west where it swamps an observed northward transport, further implicating an overly vigorous recirculation.

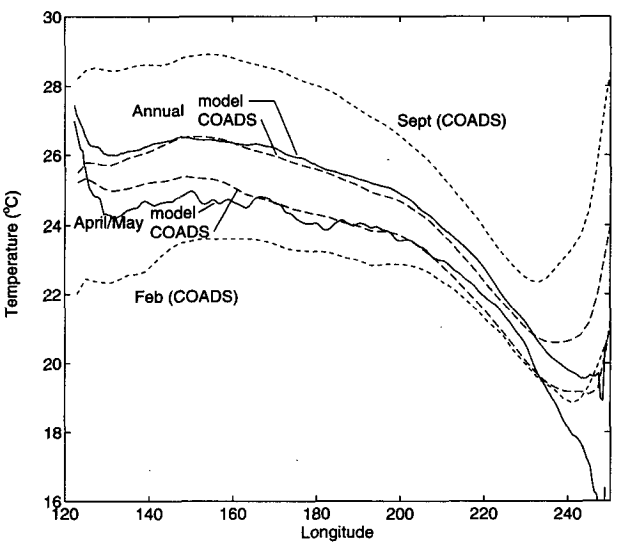

FIG. 2. Sea surface temperature along 24°N. April–May and annual mean model values (solid lines). Observed values from COADS data (Oberhuber 1988) during April–May and in the annual mean (dashed lines) and the warmest (Sep) and coolest (Feb) months (dotted lines).

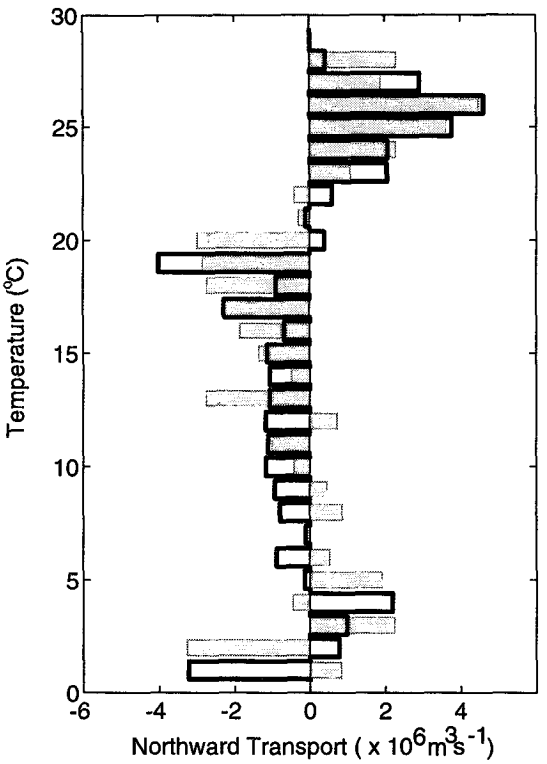

FIG. 3. Observed (heavy line) and annual mean model (shaded) northward transport across 24°N as a function of temperature. Transports are computed in 1°C temperature bins.

A comparison to Roemmich and McCallister's (1989) inversion shows the model performance in a different light (Table 3). Rather than being too strong, the return flow in the Northeast Pacific Basin east of Hawaii agrees well. This suggests that the constraint on the mass transport imposed by the presence of the Hawaii Ridge also occurs in the model solution. Further good agreement is seen in the transport west of Hawaii, to either side of 137°E, a longitude that divides areas in which the inversion requires mass conservation. However, it is the Izu Ridge, not 137°E, that marks the physical boundary between the Philippine and central Pacific basins. The Philippine Basin geostrophic transport is 37.6 Sv in the model but 56.4 Sv in the inversion due to a strong northward transport immediately west of the Izu Ridge. A large divergence in the deep layers was required to accommodate this transport (Roemmich and McCallister 1989), and we suspect that, given the model solution, this indicates locally poor performance of the inverse solution rather than any enhanced vertical mixing in the Philippine Basin. Roemmich and McCallister (1989) obtain the same heat transport as BRC, so it appears that the meridional distribution of the midocean return flow is not critical in the heat budget.

Relative to the midocean return flow, the Ekman component transports 0.34 PW (Table 2). This close agreement with observations is somewhat fortuitous, as pointed out above, because the observed value is biased toward April–May conditions. This bias partially conceals the discrepancy in model and observed mean temperature of the midocean component. Because the midocean temperature is only 0.14°C cooler than the Kuroshio, the Kuroshio contributes only 0.03 PW to the heat transport. To see why the modeled midocean temperature is so much warmer than observed we examine the meridional circulation.

d. Meridional circulation

At first glance, the annual mean model transport in temperature classes compares favorably with BRC's observations (Fig. 3). In particular, the northward transport of the warmest waters is simulated well, though there is a hint that the southward return flow is distributed over a slightly warmer temperature range. To see where the subtle errors occur that produce the poor overall heat transport, it is best to examine the temperature transport for each component (Fig. 4). The Ekman component is slightly warmer in the model due to the April–May bias of the observations. In the Kuroshio, the model transport is greater than BRC calculate but it occurs with a temperature distribution that gives it a comparable average temperature. In the midocean component, the model returns far more water southward in the 20°–25°C range than is observed. At 24°N in the model, water in this temperature range occurs between 200-m and 500-m depth, where a difference between mean model θ and climatology of 2°–4°C (Fig. 5) accounts for the approximately 3°C too warm average temperature for this component. A heat transport almost identical to BRC's value is obtained

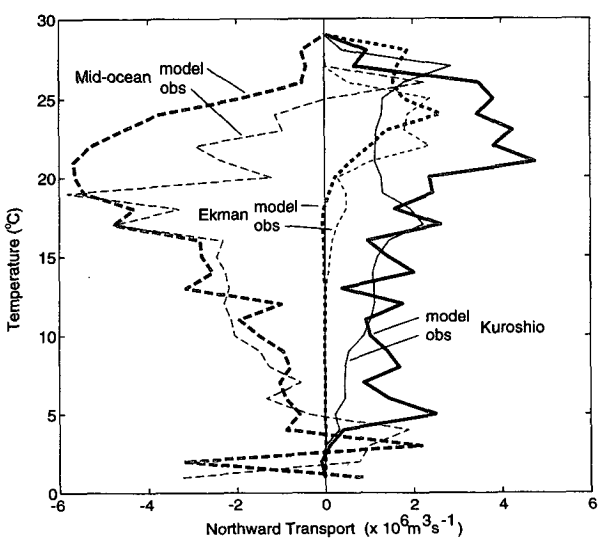

FIG. 4. Model (heavy lines) and observed (light lines) northward transport as a function of temperature for each component. Kuroshio (solid lines), Ekman (dotted lines), and midocean (dashed lines).

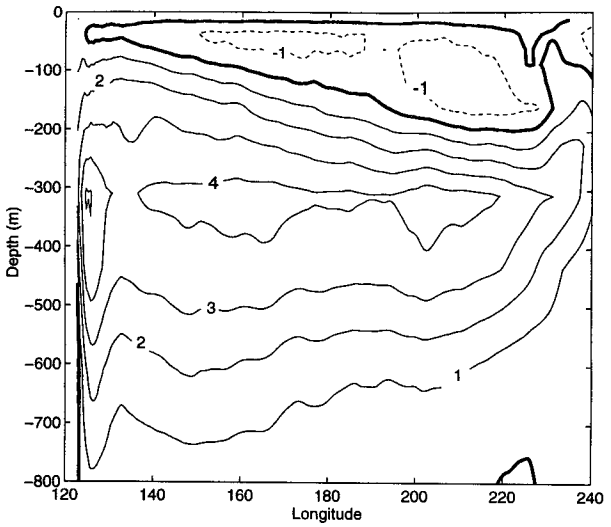

FIG. 5. Difference between model mean θ and Levitus (1982) climatology at 24°N from the surface to 800 m.

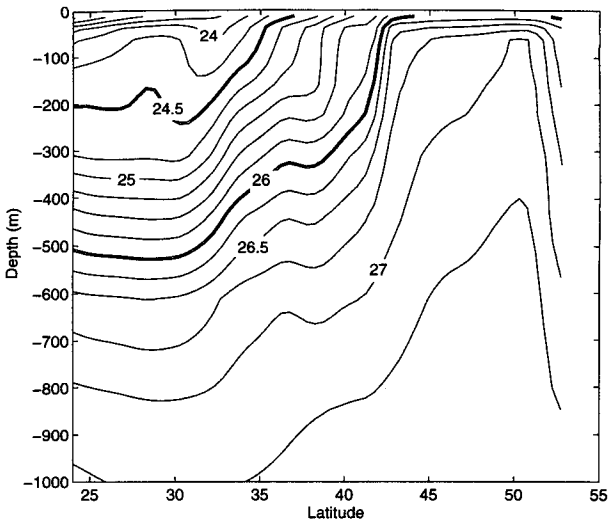

FIG. 6. Annual mean potential density in the model along 160°E in the North Pacific.

if the model velocity field is multiplied by observed θ, confirming that poor simulation of model θ in this narrow depth and temperature range of the midocean return component is responsible for the low total heat transport result. Where does this water obtain such an erroneous temperature?

At 160°E in the model (a longitude typical of meridional sections through the Kuroshio extension), isopycnals that cross 24°N at depth 200 to 500 m ($24.5 < \sigma_0 < 26$) outcrop in the region 35°–40°N (Fig. 6) where the model Kuroshio flows eastward after having separated from the coast. The water ventilated in this region forms a pycnostad approximately 150 m deep during wintertime cooling, and is returned across 24°N by advection. This return flow is too warm because the surface cooling in the Kuroshio extension is insufficient, being some 50 to 100 W m^{-2} less than observed (Fig. 7). The cooling that does occur is of order 80 W m^{-2} in this region, which the model surface boundary condition achieves through a difference in model and observed SST of roughly 2°C (80 W m^{-2} = 2°C × 40 W m^{-2} $°C^{-1}$). To obtain a further 50–100 W m^{-2} would require the model SST be greater than Levitus by 3.25–4.5°C—hardly a desirable outcome. This highlights a shortcoming of the relaxation-to-climatology surface boundary condition: the scheme cannot simulate well both observed SST and air–sea flux. Arguably, an infinitely small relaxation time could do this, but it would require the model mixed layer to be perfect.

A preferable scheme is that of Haney (1971) and Han (1984), that relaxes toward a so-called equilibrium temperature that is less (greater) than observed in regions of heat loss (gain). The relaxation timescale is determined by approximating the heat flux bulk formulae by Taylor series in the difference between SST and air temperature, and the difference between the equilibrium temperature and observed SST is proportional to the observed net heat flux and the relaxation timescale. The annual mean equilibrium temperature is less than SST in the Kuroshio by 2°–4°C (Fig. 8), just the margin required to improve the temperature of waters returned across 24°N, indicating that implementing such a surface boundary scheme in the model should lead to a much improved simulation of the ventilation process and meridional heat transport.

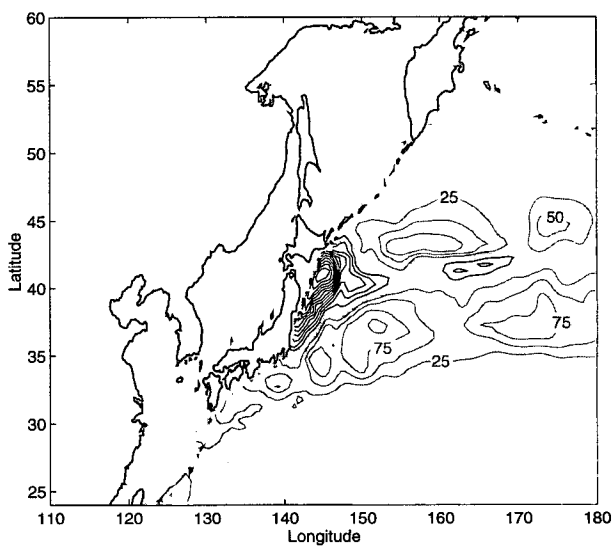

FIG. 7. Difference between observed and modeled annual mean air–sea heat loss in the Kuroshio extension region. Observed fluxes are from Oberhuber (1988). Negative values (shaded) indicate the model loses less heat than observed. Contour interval is 25 W m^{-2}.

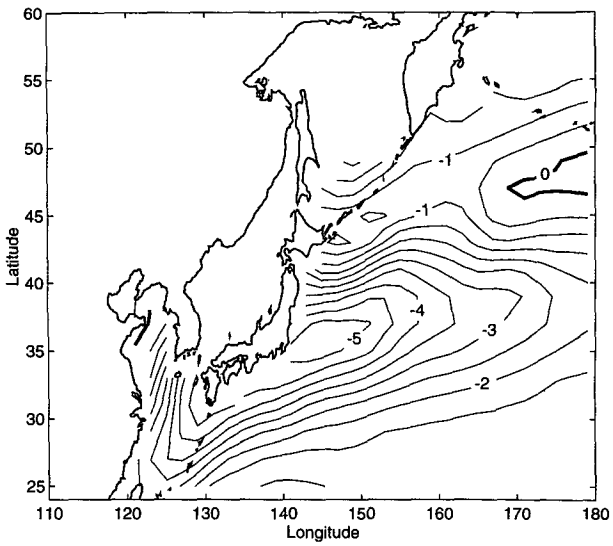

FIG. 8. Difference between the annual mean Haney equilibrium temperature and Levitus (1982) SST. The equilibrium temperature is computed from the analysis of COADS data by Oberhuber (1988).

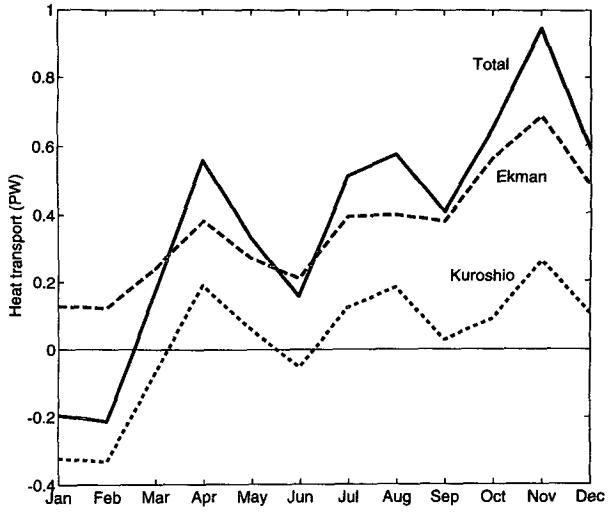

FIG. 9. Monthly model heat transport (solid line), Ekman component (dashed line), and Kuroshio component (dotted line).

4. Annual variability

a. Wind-driven changes in heat transport

BRC estimate the heat transport across 24°N has an annual variation of order 0.2 PW. This is computed by assuming variations in the northward Kuroshio and Ekman transports of about ±8 Sv are balanced by variability above 700-m depth at the temperature of the annual mean midocean component, that is, about 6°C cooler. In the model, much greater annual variability is found, ranging from 0.95 PW northward in November to 0.21 PW southward in February (Fig. 9), for a standard deviation of 0.34 PW. The variability is distributed roughly evenly between the Ekman and Kuroshio components (each ±0.2 PW), which vary in phase due to monthly variations in the temperature of the midocean component. This occurs because perturbations in the surface transport are balanced by changes in the abyssal flow below 1750 m (Fig. 10). The average temperature of the perturbation return flow is therefore considerably more than 6°C cooler than the surface flow, producing a large heat transport variation. Inspection of the abyssal velocity field shows that the abyssal transport variations are dominated by changes in the deep western boundary currents (Fig. 11). On the monthly timescale, Ekman transport variations must force rapidly propagating barotropic basin modes that balance mass by perturbing the abyssal boundary currents. The return flow for the Ekman variability therefore has a temperature close to the section average. Abyssal transport variability of a similar nature was noted at low latitudes in the North Atlantic WOCE model (Böning and Herrmann 1994) where the amplitude of the annual variability in heat transport was of the order ±1 PW. Thus, BRC's assumption that the abyssal flow is essentially steady does not hold in the model and introduces the possibility that the heat transport deduced from a single hydrographic section is much less representative of annual mean conditions than one might hope.

Observations confirm that variations in abyssal currents occur with a timescale of months (Lee et al. 1990; Niiler et al. 1993; Whitworth 1994). Though changes in the barotropic component of the deep western boundary in the Atlantic observed by Lee et al. (1990) could not be explained in terms of an instantaneous Sverdrup balance with monthly winds, they did not

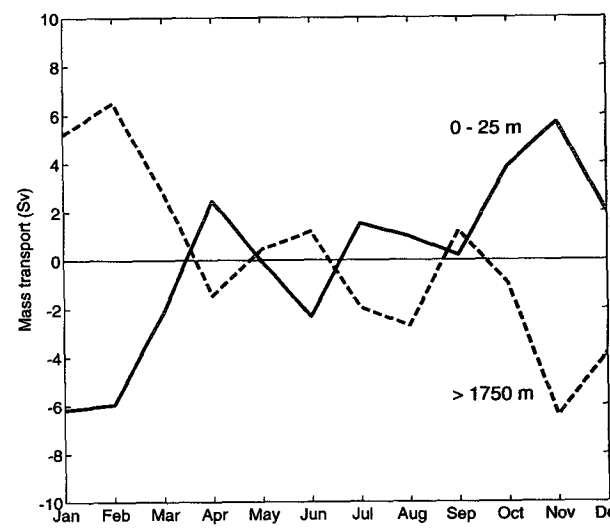

FIG. 10. Mass transport by month in selected layers of the model, minus the annual mean. From the surface to 25-m depth (solid line) and from 1750-m depth to the seafloor (dashed line).

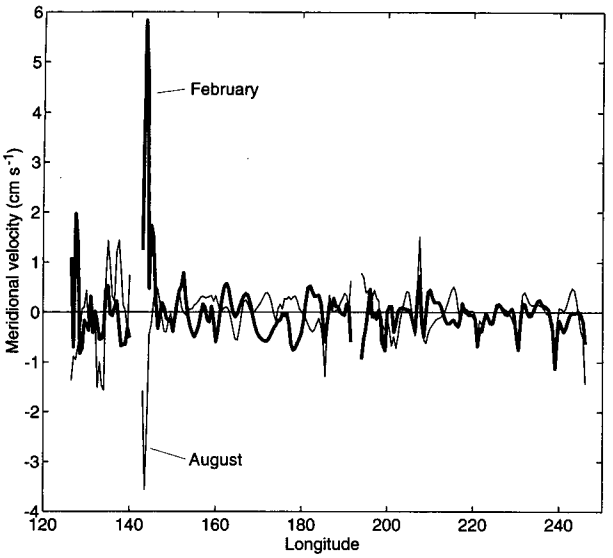

FIG. 11. Model meridional velocity at 24°N at 3000-m depth in February (heavy solid line) and August (light solid line). The largest variation occurs within the deep western boundary current on the eastern side of the Izu Ridge at 142°E.

attempt a comparison to zonally integrated Ekman transport variation.

b. *Accounting for variability in observations*

To calculate transports from hydrographic data, assumptions must be made regarding referencing the geostrophic velocities. The likely influence on the total heat transport of BRC's assumptions can be examined by recomputing the model heat transport as if the mass transport were referenced according to BRC's procedure. Where the 24°N section crossed the Kuroshio, BRC referenced velocities to shipboard Doppler profiler data in depths less than 1000 m. Elsewhere they used a deep reference level of 3000 m or the seafloor. Closure of the mass budget was made by applying a uniform velocity adjustment across the entire section. In our "simulated BRC" analysis, we compute for each month a modified velocity field by (i) in deep water, subtracting the model velocity at 3000-m depth from all depths in the water column, (ii) in water between 1000 and 3000 m deep, subtracting the bottom velocity, and (iii) leaving the model velocity unchanged in shallower water. In each month, the Ekman transport due to the monthly winds is removed and replaced by the annual mean Ekman transport. Depending on the month, the misclosure of the mass transport required uniform velocity adjustments of between -2.2×10^{-5} and 4×10^{-4} m s^{-1}, similar to the 1.9×10^{-4} m s^{-1} applied by BRC. Figure 12 shows the heat transport computed by multiplying the new velocity by the original monthly temperatures (dashed line). The result is very close to the original model heat transport in each month, indicating that the reference level assumptions have little impact on the estimated heat transport. But the large monthly variation remains despite having adjusted the Ekman mass transport to annual mean conditions.

It was noted in section 3c that using surface temperatures observed during a single hydrographic section could seasonally bias the Ekman component of the heat transport estimate. Figure 12 shows the magnitude of the possible bias, with a "virtual cruise" through the model ocean potentially returning a heat transport anywhere between −0.1 and 0.8 PW depending on the month. Interestingly, the model transport during April–May is very close to the annual mean value, so that a "virtual cruise" through the model ocean at this time of year would, by chance, return a heat transport close to the true annual value.

A more robust procedure for getting the correct value would be to adjust the surface temperatures to make them representative of annual mean conditions, just as the Ekman mass transport was adjusted by BRC. We test the effectiveness of this by computing the heat transport in each month using the adjusted velocity computed above and the monthly temperature for the Kuroshio and midocean components, except using the annual-mean surface layer temperature when computing the Ekman component. The heat transport by this procedure (Fig. 12 dotted line) varies much less from month to month (standard deviation 0.013 PW) and is indeed a less biased estimator of the annual mean.

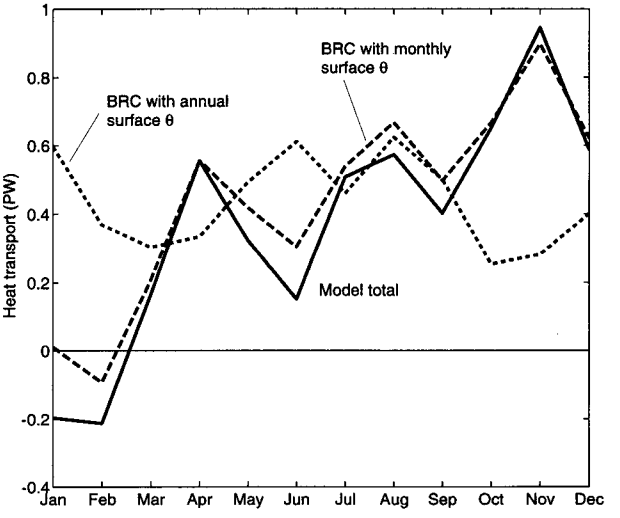

FIG. 12. Assumptions of the BRC analysis procedure applied to the model results. Monthly heat transport when the model velocity field is adjusted using the same reference level assumptions as BRC (dashed line). Monthly heat transport when the model velocity field is adjusted, and the annual mean temperature of the surface layer, rather than the monthly value, is used in computing the Ekman component (dotted line). True monthly model heat transport (solid line).

5. Other features of the model circulation

a. Kuroshio Current separation

Contrary to observations, not all of the model Kuroshio transport separates from the coast at 35°N. Some 15 Sv of warm subtropical water continues northward adjacent to the coast into a region where the Levitus climatology shows relatively cool SST. As a result, intense surface cooling peaking at 300 W m^{-2} occurs in the boundary current. While this does not occur over a large enough area to significantly affect the heat budget, it does produce a 200-m deep thermostad that invades the region east of Japan to 170°W. The thermostad is capped by a warm surface layer from July to November but is ventilated throughout the remainder of the year. This feature of the circulation, a direct result of the poor Kuroshio separation, is quite unrealistic, but we are uncertain whether it adversely affects the simulation of the North Pacific heat budget.

b. Abyssal circulation

The model abyssal circulation is dominated by deep boundary currents (adjacent to bathymetric features) connected by zonal jets (Semtner and Chervin 1992, Plate 2). Abyssal flow occurring via a sinuous network of narrow currents is different from the view implied by the fixed reference level calculations of BRC and Roemmich and McCallister (1989) that do not allow for different reference levels within deep western boundary currents. This may account partly for the poor agreement of the distribution of transport within individual basins in Table 3. Without observations to support the occurrence of deep zonal jets, the realism of this feature of the model solution is open to question.

Integrated over depth from 710 m to the seafloor, the deep relaxation to observed θ produces a cooling equivalent to 2.1 W m^{-2} in the area from 24° to 55°N. Though small compared to surface fluxes, this accounts for a steady heat loss of 0.06 PW, or roughly 15% of the transport across 24°N. North of 55°N, the deep relaxation applied at all depths amounts to a parameterization of convection and water mass formation in the Aleutian Basin and Gulf of Alaska. In this region, the cooling averages 31 W m^{-2} and removes a further 0.07 PW from the North Pacific. Arguably, as a parameterization of convection, the deep relaxation north of 55°N may be considered part of the surface flux, and we include it as such in reporting the model meridional heat transport in Fig. 1.

In agreement with BRC, we find that the circulation below 800 m contributes little to the heat transport across 24°N and infer from this that the deep cooling is balanced either by subgrid-scale diffusion or a weak drift in the deep θ. There is no suggestion that it is balanced by advection across 24°N. Therefore, while recognizing that there are possible shortcomings in the model's representation of the deep circulation, we see no reason to suspect that these compromise our conclusions concerning the upper ocean circulation that dominates North Pacific heat transport.

c. Mesoscale eddies

BRC estimate the contribution to the heat transport by mesoscale eddies to be of order 0.1 PW southward. The model also shows a southward sense to the eddy component, but of order 0.01 PW (Table 1). A comparison of the model with Geosat altimeter observations (Wilkin and Morrow 1994) in the Southern Ocean showed midlatitude model eddy kinetic energy is typically 10 times weaker than observed. Therefore, the simulated eddy heat transport in the North Pacific could easily be too low by an order of magnitude. We see no reason, on the basis of the present model results, to disagree with BRC's estimate of the likely contribution of eddies. Higher resolution models and better altimeter data will help indicate when models are approaching realistic levels of eddy heat transport.

6. Discussion and summary

The model heat transport across 24°N in the Pacific is half that of recent observational estimates. This is clearly the result of the model surface heat flux boundary condition, and future model performance could be easily improved with a better heat flux parameterization. This hypothesis will be tested in forthcoming runs of a 1/4° resolution version of the model using surface heat flux parameterizations based on the Haney and Han methods.

In other respects, the model captures well the mechanisms of meridional heat transport. By having available the results from 5 years of simulation we are able to conclude several results regarding the effect of variability on meridional heat transport estimates.

The Kuroshio Current exhibits interannual variations that make an appreciable contribution to the overall heat budget. Since the model contains no interannual forcing, this feature of the solution must result from nonlinear processes in the Kuroshio Current or its recirculation. On an interannual basis the Kuroshio recirculation is observed to switch between two mean states commonly referred to as "straight path" and "meander path" with net transports that differ by some 10 Sv (Qiu and Joyce 1992). We would not claim here that the model solution reproduces the recognized features of these straight-path and meander-path states. However, the role of interannual variation in the model heat transport does suggest that a net contribution to the North Pacific heat budget may result from interannual variation in the Kuroshio system and that some attempt should be made to compute this (such as from the data of Qiu and Joyce 1992) to augment the estimate of the steady circulation by BRC.

Far from being essentially steady, as assumed by BRC, the model abyssal circulation exhibits consid-

erable monthly variation. As a result, direct heat transport estimates from single hydrographic sections should admit the possibility that short timescale variations in the Ekman transport tend to be returned at the section average temperature rather than the annual mean transport-weighted temperature of the midocean flow. Because of the large variation in the monthly heat transport that this variability produces, some care is required in making adjustment for seasonal variability in the Ekman component. Not only should the annual mean Ekman mass transport be considered, but so too should the annual mean Ekman layer temperatures. This is problematic because, while SST is observed with good temporal coverage, in general, temperatures throughout the Ekman layer are not. This emphasizes the value of repeated sampling of the upper ocean thermal structure by XBT surveys.

Due to the perhaps fortuitous timing of the 24°N hydrographic section in April–May, when the seasonal bias of the model solution is small, we would not, on the basis of the model results, suggest any revision to the estimate by BRC that the North Pacific heat transport at 24°N is 0.76 ± 0.3 PW.

The comparison of the model midocean transports to those of Roemmich and McCallister's (1989) inverse solution suggested that the inverse method successfully placed constraints similar to those of the model geometry on the oceanic mass budget. An inversion of the North Pacific circulation using the additional hydrographic sections occupied as a part of WOCE will doubtless give a more tightly constrained solution and will likely lead to a reduction of the errors that BRC estimate for the components of the mass budget across their single section. An inverse method that merges upper ocean thermal data by objective analysis should also reduce the problem of the seasonal bias in a single section, and ultimately provide probably the most accurate estimate of oceanic meridional heat transport.

Acknowledgments. We are grateful to A. Semtner and R. Chervin for making available the results of their model simulation performed at the National Center for Atmospheric Research. T. Bettge and M. McCann were of great assistance in our initial inspection of the model output using the Ocean Processor at NCAR. NCAR is funded by the National Science Foundation. We thank J. Church and T. McDougall for helpful discussions throughout the project. This work contributes to the CSIRO Climate Change Research Program. The authors are funded by Australia's National Greenhouse Research Program.

REFERENCES

Bingham, F. M., and L. D. Talley, 1991: Estimates of Kuroshio transport using an inverse technique. *Deep-Sea Res.*, **38**(Suppl. 1), S21–S43.

Böning, C. W., and P. Herrmann, 1994: Annual cycle of poleward heat transport in the ocean: Results from high-resolution modeling of the North and Equatorial Atlantic. *J. Phys. Oceanogr.*, **24,** 91–107.

Bryan, K., 1962: Measurements of meridional heat transport by ocean currents. *J. Geophys. Res.*, **67,** 3403–3413.

Bryden, H. L., 1993: Ocean heat transport across 24°N latitude. *Interactions Between Global Climate Subsystems and the Legacy of Hann,* G. A. McBean, Ed., Amer. Geophys. Union, 65–75.

——, D. H. Roemmich, and J. A. Church, 1991: Ocean heat transport across 24°N in the Pacific. *Deep-Sea Res.*, **38,** 297–324.

Esbensen, S. K., and Y. Kushnir, 1981: Heat budget of the global ocean: Estimates from surface marine observations. Climatic Research Institute, Oregon State University, Report No. 29, Corvallis, OR, 223 pp.

Hall, M. M., and H. L. Bryden, 1982: Direct estimates and mechanisms of ocean heat transport. *Deep-Sea Res.*, **29,** 339–359.

Han, Y.-J., 1984: A numerical world ocean general circulation model. Part II. A baroclinic experiment. *Dyn. Atmos. Oceans,* **8,** 141–172.

Haney, R. L., 1971: Surface thermal boundary condition for ocean circulation models. *J. Phys. Oceanogr.*, **1,** 241–248.

Hastenrath, S., 1980: Heat budget of tropical ocean and atmosphere. *J. Phys. Oceanogr.*, **10,** 159–170.

Hellerman, S., and M. Rosenstein, 1983: Normal monthly wind stress over the World Ocean with error estimates. *J. Phys. Oceanogr.*, **13,** 1093–1104.

Lee, T. N., W. Johns, F. Schott, and R. Zantopp, 1990: Western boundary current structure and variability east of Abaco, Bahamas, at 26.5°N. *J. Phys. Oceanogr.*, **1990,** 446–466.

Levitus, S., 1982: *Climatological Atlas of the World Ocean.* NOAA Prof. Paper No. 13, U.S. Govt. Printing Office, 183 pp.

McBean, G. A., 1991: Estimation of the Pacific Ocean meridional heat flux. *Atmos.–Ocean,* **29,** 576–595.

McCann, M. P., A. J. Semtner Jr., and R. M. Chervin, 1994: Transports and budgets of volume, heat, and salt from a global eddy-resolving ocean model. *Climate Dyn.*, **10,** 59–80.

Niiler, P. P., J. Filloux, W. T. Liu, R. M. Samelson, J. D. Paduan, and C. A. Paulson, 1993: Wind-forced variability of the deep eastern North Pacific: Observations of seafloor pressure and abyssal currents. *J. Geophys. Res.*, **98,** 22 589–22 602.

Oberhuber, J. M., 1988: An atlas based on the COADS data set: The budgets of heat, buoyancy and turbulent kinetic energy at the surface of the global ocean. Report 15, Max Planck Institut fur Meteorologie, 19 pp. plus figs.

Qiu, B., and T. M. Joyce, 1992: Interannual variability in the mid- and low-latitude western North Pacific. *J. Phys. Oceanogr.*, **22,** 1062–1079.

Roemmich, D. H., and T. McCallister, 1989: Large scale circulation of the North Pacific Ocean. *Progress in Oceanography,* Vol. 22, Pergamon, 171–204.

Semtner, Jr., A. J., and R. M. Chervin, 1992: Ocean general circulation from a global eddy-resolving model. *J. Geophys. Res.*, **97,** 5493–5550.

Talley, L. D., 1984: Meridional heat transport in the Pacific Ocean. *J. Phys. Oceanogr.*, **14,** 231–241.

Trenberth, K. E., and A. Solomon, 1994: The global heat balance: Heat transports in the atmosphere and ocean. *Climate Dyn.*, **10,** 107–134.

Whitworth, T., 1994: Deep flow in the southwest Pacific. U.S. WOCE Implementation Report No. 6, U.S. WOCE Office, College Station, TX, 48 pp.

Wilkin, J. L., and R. A. Morrow, 1994: Eddy kinetic energy and momentum flux in the Southern Ocean: Comparison of a global eddy-resolving model with altimeter, drifter and current-meter data. *J. Geophys. Res.*, **99,** 7903–7916.